Conditional Müller Cell Ablation Leads to Retinal Iron Accumulation

Bailey Baumann,[1] Jacob Sterling,[1] Ying Song,[1] Delu Song,[1] Marcus Fruttiger,[2] Mark Gillies,[3] Weiyong Shen,[3] and Joshua L. Dunaief[1]

[1]F.M. Kirby Center for Molecular Ophthalmology, Scheie Eye Institute, Perelman School of Medicine at the University of Pennsylvania, Philadelphia, Pennsylvania, United States
[2]Institute of Ophthalmology, University College London, London, United Kingdom
[3]Save Sight Institute, The University of Sydney, Sydney, Australia

Correspondence: Joshua L. Dunaief, F.M. Kirby Center for Molecular Ophthalmology, Scheie Eye Institute, Perelman School of Medicine at the University of Pennsylvania, 305 Stellar-Chance Laboratory, 422 Curie Boulevard, Philadelphia, PA 19104, USA;
jdunaief@upenn.edu.

Submitted: February 24, 2017
Accepted: July 7, 2017

Citation: Baumann B, Sterling J, Song Y, et al. Conditional Müller cell ablation leads to retinal iron accumulation. *Invest Ophthalmol Vis Sci*. 2017;58:4223–4234. DOI:10.1167/iovs.17-21743

Purpose. Retinal iron accumulation is observed in a wide range of retinal degenerative diseases, including AMD. Previous work suggests that Müller glial cells may be important mediators of retinal iron transport, distribution, and regulation. A transgenic model of Müller cell loss recently demonstrated that primary Müller cell ablation leads to blood–retinal barrier leakage and photoreceptor degeneration, and it recapitulates clinical features observed in macular telangiectasia type 2 (MacTel2), a rare human disease that features Müller cell loss. We used this mouse model to determine the effect of Müller cell loss on retinal iron homeostasis.

Methods. Changes in total retinal iron levels after Müller cell ablation were measured using inductively coupled plasma mass spectrometry. Corresponding changes in the expression of iron flux and iron storage proteins were determined using quantitative PCR, Western analysis, and immunohistochemistry.

Results. Müller cell loss led to blood–retinal barrier breakdown and increased iron levels throughout the neurosensory retina. There were corresponding changes in mRNA and/or protein levels of ferritin, transferrin receptor, ferroportin, Zip8, and Zip14. There were also increased iron levels within the RPE of retinal sections from a patient with MacTel2 and both RPE and neurosensory retina of a patient with diabetic retinopathy, which, like MacTel2, causes retinal vascular leakage.

Conclusion. This study shows that Müller cells and the blood–retinal barrier play pivotal roles in the regulation of retinal iron homeostasis. The retinal iron accumulation resulting from blood–retinal barrier dysfunction may contribute to retinal degeneration in this model and in diseases such as MacTel2 and diabetic retinopathy.

Keywords: retina, iron, Zip8, Zip14, ferroportin, Müller cells, blood–retinal barrier, AMD, macular telangectasia type 2, diabetic retinopathy

Iron is necessary for cell survival, serving as an essential cofactor in numerous cellular and biochemical processes. However, intracellular ferrous iron accumulation can catalyze Fenton chemistry, leading to oxidative stress and cell death in iron-loaded tissues.[1] The retina is particularly vulnerable to oxidative assault due to factors such as its high metabolic rate, high oxygen tension, and a high concentration of polyunsaturated fatty acids. Intracellular retinal iron accumulation is implicated in the development and exacerbation of neurodegenerative diseases, including AMD, the leading cause of irreversible blindness in developed nations in individuals over the age of 50.[2,3] Unfortunately, there are large gaps in our understanding of retinal iron homeostasis and the mechanisms of iron dysregulation in retinal neurodegenerative diseases. A thorough study of the role of specific retinal cells in the transport of iron across the retina will allow for a more complete picture of the pathogenesis of retinal disease involving iron dysregulation.

Müller cells, the principal glial cell of the retina, perform a diverse range of functional and supportive roles for the surrounding retinal neurons, including maintaining homeostasis of the neuronal microenvironment, providing nutritional support, and removing metabolic waste.[4,5] Müller cell loss or dysfunction has been observed in several retinal diseases including macular telangiectasia type 2 (MacTel2) and diabetic retinopathy (DR).[6–10] Patients with both diseases have vascular pathology and photoreceptor degeneration. Additionally, Müller cell remodeling is seen in transgenic models of retinal degenerative disease.[11,12] These data indicate that Müller cells are essential for the maintenance of normal retinal morphology and function. However, the downstream consequences of Müller cell loss or dysfunction and the connection between Müller cell loss and retinal degeneration are not well understood.

A study by Shen et al.[13] demonstrated that primary Müller cell loss results in vascular leakage, neovascularization, and photoreceptor degeneration. This model suggests that Müller cell dysfunction may be an important upstream cause of the vascular pathology and retinal degeneration seen in human retinal diseases such as MacTel2. Similarly, a recently identified

spontaneous mutation in the Brown Norway from Janvier rat strain (BN-J), which has Müller cell loss, develops retinal telangiectasia and degeneration resembling human MacTel2.[14] The transgenic model of Müller dysfunction developed by Shen et al.[13] was used in this study to explore the role of Müller cells in retinal iron regulation.

Müller cells play several essential roles in ensuring proper retinal function. Two of those essential functions, formation and maintenance of the blood–retinal barrier (BRB)[15,16] and production of the iron regulatory hormone, hepcidin,[17] may play a central role in regulating the flow of iron into the retina. In this study, we will determine if Müller cell loss or dysfunction leads to changes in retinal iron levels and whether these changes occur as a result of loss of BRB integrity and/or changes in retinal hepcidin production.

In vascularized retinas of both humans and rodents, Müller cell processes surround the endothelium of blood vessels within the three capillary beds of the inner retina. Disruption of the BRB compromises the integrity of the retinal microenvironment, upsetting the carefully regulated flux of nutrients and waste in and out of the retina. Furthermore, BRB disruption results in vascular leakage and edema, two pathologies found in a number of retinal diseases, including MacTel2 and DR.[16] The importance of Müller cells in inner BRB formation and maintenance suggests that Müller cells, along with the endothelial cells of the retinal vasculature, create a physical barrier to prevent the unregulated flux of iron into the retina. When Müller cells are dysfunctional or absent, the barrier function of endothelial cells alone may not be sufficient to properly regulate retinal iron entry.

Müller cells are also producers of the iron regulatory peptide hormone, hepcidin.[17] Hepcidin negatively regulates the cell-membrane expression of the only known mammalian iron exporter, ferroportin (Fpn).[18] If Müller cells are the predominant producers of retinal hepcidin, a decrease in the number of functional Müller cells may lead to a decrease in hepcidin production. Our lab has previously demonstrated that there is retinal iron accumulation in mice that have a hepcidin-resistant mutant form of Fpn[19] and in hepcidin knockout mice.[20] These data suggest that Müller cell loss, and a potential decrease in hepcidin production, may lead to the same iron accumulation phenotype. The loss of hepcidin would lead to increased Fpn protein on the abluminal membrane of the retinal endothelial cells, leading to increased import of iron into the retina.

Retinal iron dysregulation in response to Müller cell dysfunction may contribute to the retinal degeneration observed in individuals with diseases such as MacTel2 and DR. Evidence of retinal iron dysregulation in DR has already been demonstrated by increased iron levels in the vitreous of patients[21,22]; however, the contribution of Müller cells in this process has not been explored. Currently, the consequences of Müller cell loss or dysfunction within the retina of these patients is unknown, but iron accumulation following Müller cell loss may represent one pathway that leads to the exacerbation of retinal degeneration.

In this study, we test the hypothesis that Müller cell loss leads to retinal iron dysregulation using the Müller cell ablation (MCA) mouse model developed by Shen et al.[13] We show that Müller cell loss or dysfunction results in increased retinal iron levels and altered mRNAs and proteins involved in iron storage, import, and export. These results indicate that Müller cells play an important role in the maintenance of retinal iron homeostasis. Furthermore, as these MCA mice model human MacTel2, we used the Perls' stain to detect elevated iron levels in postmortem human MacTel2 and DR retinas compared to healthy age-matched controls, suggesting that iron accumulation in response to Müller cell dysfunction may contribute to subsequent retinal degeneration.

Materials and Methods

Generation of MCA (Rlbp-CreER-DTA176) Mice

MCA (Rlbp-CreER-DTA176) mice were produced using the regulatory region of *Rlbp1* as a Müller cell–specific promoter along with the Cre-LoxP system.[13] Rlbp is also expressed in RPE cells, but Cre expression is restricted to Müller cells in this transgenic model. Rlbp1-CreER mice were crossed with Rosa-DTA176 mice, which resulted in Rlbp-CreER-DTA176 transgenic mice that were suitable for conditional MCA. Mice crossed with the Rosa-*LacZ* reporter strain were used as controls. *DTA176* gene expression was induced by daily intraperitoneal injection of tamoxifen (TMX; 3 mg in 0.2 mL sunflower oil) for 4 consecutive days at approximately 6 to 8 weeks of age. Mice were either killed 2 weeks (2-week MCA, 2-week control) or 5 months (5-month MCA, 5-month control) after TMX injection. Both the MCA and control mice were of CBA/CaH × C57BL/6J mixed background, and both males and females were used in this study. All mice were negative for the *rd8* allele.

Inductively Coupled Mass Spectrometry

Samples were analyzed for iron, copper, and zinc using an inductively coupled mass spectrometer (Nexion 300D; Perkin Elmer, Shelton, CT, USA) at the PADLS New Bolton Center Toxicology Laboratory, University of Pennsylvania, School of Veterinary Medicine (Kennett Square, PA, USA) as described previously.[23]

Cryosection Immunofluorescence

Eyes were fixed in 4% paraformaldehyde for 5 minutes and then anterior segments were removed to form an eyecup. After post fixation in 4% paraformaldehyde for 1 hour, eyecups were transferred to PBS containing 30% sucrose and then embedded in optimal cutting temperature (OCT) compound. Immunohistochemistry was performed on 10-μm thick cryosections, as described previously.[20] Antibodies used were mouse anti-glutamine synthetase (1:500; Abcam, Cambridge, UK); rabbit anti-light ferritin (E17) (1:200; a gift from P. Arosio, University of Brescia, Italy); goat anti-albumin (1:100; Betyl Laboratories, Montgomery, TX, USA); rat anti-transferrin receptor (1:200; Serotec, Kidlington, UK); and rat anti–glial fibrillary acidic protein (anti-GFAP) (1:500; Abcam). Control sections were treated identically but with omission of primary antibody. Sections were analyzed by fluorescence microscopy using identical exposure parameters across genotype using Nikon Elements software (Nikon Instruments, Melville, NY, USA). Pixel density analysis of the L-ferritin (Ft-L) stain was completed using an open source image-processing package (FIJI software).[24]

Quantitative Real-Time PCR

RNA isolation was performed (RNeasy Kit; Qiagen, Valencia, CA, USA) according to the manufacturer's protocol. cDNA was synthesized with reverse transcription reagents (TaqMan; Applied Biosystems, Darmstadt, Germany) according to the manufacturer's protocol. Gene expression of *glu1*, *tfrc*, *slc11a2*, *cp*, *heph*, *fpn*, *hamp*, *slc39a8*, and *slc39a14* was analyzed using quantitative real-time (RT) PCR as previously published.[20] Gene expression assays (TaqMan; Applied Biosystems, Foster City, CA, USA) were used for PCR analysis. GAPDH served as an internal control. Real-time RT-PCR was performed on a commercial sequence detection system (ABI Prism 7500; Applied Biosystems, Darmstadt, Germany). All reactions were performed in

technical triplicates ($N = 3$–5 mice per genotype). Probes used were as follows: *zip8* (*slc39a8*, Mm00470855_m1), *zip14* (*slc39a14*, Mm01317439_m1), *tfrc* (Mm00441941), *hamp* (Mm00519025), *cp* (Mm00432654), *heph* (Mm00515970), *fpn* (Slc40a1, Mm00489837), *dmt1* (*slc11a2*, Mm00435363), *glul* (Mm00725701).

Neurosensory Retinal Protein Extraction and Western Blotting

Neurosensory retina protein lysates were extracted using Laemmli SDS lysis buffer supplemented with protease/phosphatase inhibitor mixture and phenylmethylsulfonyl fluoride (PMSF) (Cell Signaling Technology, Danvers, MA, USA). Lysates were treated and run as described previously.[25] Imaging was done using GE Amersham Imager 600 (GE Healthcare, Chalfont St. Giles, UK). FIJI software was used for band densitometry.[24] Primary antibodies used were as follows: rat anti-transferrin receptor (Serotec), rabbit anti-Dmt1 (NRAMP24-A; Alpha Diagnostic International, San Antonio, TX, USA), rabbit anti-Zip8 (ThermoScientific, Philadelphia, PA, USA), rabbit anti-Zip14 (ThermoScientific), rabbit anti-Fpn (Pierce, Chicago, IL, USA), rabbit anti-ferritin (E17) (P. Arosio), and mouse anti-beta actin (ab8226; Abcam). Secondary antibodies used were as follows: IRDye 680RD donkey anti-rabbit (LI-COR P/N 926-68072), donkey anti-mouse (LI-COR P/N 925-68070), and donkey anti-rat (LI-COR P/N 925-68076). All primary antibodies were used at a 1:1000 dilution and all secondary antibodies were used at a 1:5000 dilution. β-Actin served as an internal control.

Human Retinal Tissue

Postmortem eyes from three donors were obtained in accordance with the Declaration of Helsinki and fixed in formalin. Strips of retina/choroid/sclera containing the macular region were dissected and embedded in paraffin. The normal eye donor was from a 61-year-old Caucasian man who died of lung cancer. The MacTel2 donor was a 61-year-old woman who died of respiratory failure. She had typical telangiectatic macular vessels and diffuse late leakage in the temporal macula on a fluorescein angiogram. Her case has been reported previously.[7] The DR donor was a 70-year-old man. He had documented macular edema, for which he received intravitreal Lucentis injections.

Perls' Staining for Iron

Paraffin was removed from the sections, which were rehydrated through xylenes and descending ethanol and washed in distilled water. Slides were then put into Coplin jars containing 2.5% potassium ferric ferrocyanide and 2.5% hydrochloric acid solution. Closed Coplin jars were heated in a nonshaking 65°C water bath under a fume hood for 45 minutes. Afterward, slides were again washed in distilled water. Sensitivity for iron detection was enhanced by subsequent incubation of tissue in purple peroxidase substrate for 25 minutes at room temperature (VIP; Vector Laboratories, Inc., Burlingame, CA, USA). Slides were then washed in 1× PBS. Slides were examined on a Nikon Eclipse 80i microscope (Nikon Instruments), and images were acquired using NIS-BR Elements software (version 4.1; Nikon Instruments).

Statistical Analysis

Mean ± standard error of the mean was calculated for each group. Student's two-group, two-tailed *t*-test was used for statistical analysis of relative mRNA, pixel density, and band densitometry levels. All statistical analyses were performed using GraphPad Prism 5.0 (San Diego, CA, USA).

Results

Characterization of MCA Experimental Mice

To verify that the MCA mice studied herein had primary Müller cell loss as described in Shen et al.,[13] we characterized the changes in the retina of 2-week and 5-month MCA Rlbp-CreER-DTA176 experimental mice compared with age and strain-matched controls (2-week and 5-month control). The 2-week MCA mice and the 2-week controls were 10 weeks old when studied, while the 5-month MCA and the 5-month control mice were 7 months of age when studied. MCA resulted in a reduction in the mRNA levels of Müller cell–specific markers, retinal disorganization, an increase in Müller cell stress, and disruption of the inner BRB. There was a decrease in the mRNA levels of the Müller cell–specific marker, glutamine synthetase (Glul), in the 5-month MCA retina compared with the 5-month control, consistent with loss or dysfunction of Müller cells (Fig. 1A). Additionally, immunohistochemistry (IHC) for glutamine synthetase (GS) revealed focal loss of Müller cells in the 2-week (Fig. 1D) and 5-month MCA retinas (Fig. 1F) and retinal disorganization at the retinal outer limiting membrane, which is formed by Müller cell endfeet, as demonstrated by photoreceptor nuclei protrusion into the subretinal space in the 2-week MCA retina (Fig. 1D). The MCA mice also had upregulation of GFAP in the Müller cells at both 2 weeks (Fig. 1I) and 5 months post ablation (Fig. 1K). Upregulation of GFAP in Müller cells is an indicator of Müller cell stress.[26] In Shen et al.,[13] the authors demonstrated, using fundus fluorescein angiography, that primary MCA led to BRB breakdown beginning 12 days post ablation. We verified this finding in the mice studied herein by determining the localization of albumin in the retina of the experimental and control mice. Albumin does not freely pass through the BRB and should typically be confined to the blood vessels within the neurosensory retina. In the 2-week (Fig. 1N) and 5-month (Fig. 1P) MCA retinas, there was diffuse localization of albumin throughout the neurosensory retina that was not confined to the blood vessels, while albumin was confined to the blood vessels in the 2-week (Fig. 1M) and 5-month (Fig. 1O) control retinas.

Primary MCA Leads to Intracellular Iron Accumulation in the Neurosensory Retina

We determined how retinal iron levels were altered with MCA using both direct measurements of retinal iron levels with inductively coupled mass spectrometry (iCP-MS), as well as indirect measures of intracellular iron by comparing the mRNA and protein levels of the iron-regulated proteins between the MCA and control neurosensory retinas.

We found iron accumulation in the neurosensory retina of both the 2-week and 5-month MCA mice compared with age-matched controls. When measured by iCP-MS, there was an increase in iron levels within the neurosensory retina of the 5-month MCA mice compared with 5-month controls (Fig. 2A). Retinal iron levels were also indirectly assessed by the protein levels of the cytosolic iron storage protein, Ft-L. Protein levels of Ft-L are controlled by intracellular iron levels through posttranscriptional regulation by the iron regulatory proteins 1 (IRP1) and IRP2; an increase in intracellular iron levels leads to a decrease in binding of IRP1 or IRP2 to the 5′ iron responsive element (IRE) on the Ft-L mRNA, allowing translation and increased intracellular Ft-L protein levels.[27] Consistent with the

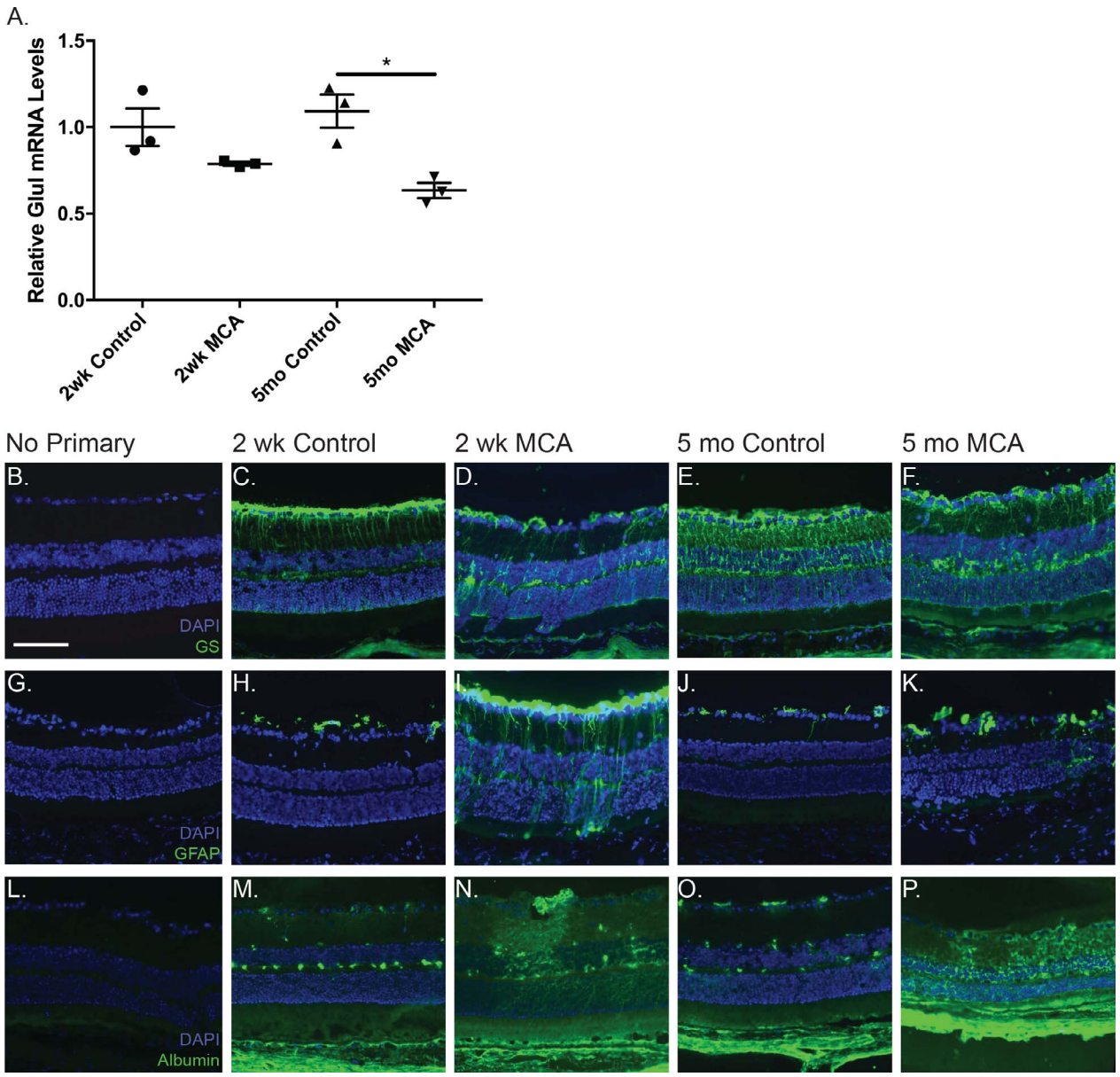

Figure 1. Characterization of MCA experimental mice. Scatterplot showing relative Glul mRNA levels by quantitative PCR analysis in the neurosensory retina. There is a significant decrease in Glul mRNA levels in the 5-month MCA neurosensory retina compared to age-matched controls and a trend toward a decrease in Glul mRNA levels in the 2-week MCA neurosensory retina compared to age-matched controls (**A**). Statistical analysis was performed using Student's two-group, two-sided *t*-test. $^{*}P < 0.05$. $N = 3$ retinas per group. Immunofluorescence for Glul demonstrated patchy Müller cell loss and protrusion of photoreceptor nuclei into the subretinal space in the 2-week (**D**) and 5-month MCA (**F**) retinas compared to age-matched controls (**C**, **E**). There is an increase in GFAP staining of Müller cells in both the 2-week MCA (**I**) and 5-month MCA (**K**) retinas compared to age-matched controls (**H**, **J**). Immunofluorescence for albumin in the neurosensory retina was performed to determine whether the blood–retinal barrier was intact. There is diffuse albumin staining in the 2-week MCA (**N**) and 5-month MCA (**P**) neurosensory retinas, while albumin was confined to the blood vessels in the age-matched controls (**M**, **O**). One representative photomicrograph is shown for each group in each set of images. *Scale bars*: 100 μm.

increase in iron levels within the 5-month MCA retina, we found that there was an increase in Ft-L protein in the neurosensory retina of the 5-month MCA mice compared with 5-month controls, as assessed by Western analysis (Fig. 2B). Additionally, we used Ft-L immunolabeling to determine whether MCA resulted in a change in the distribution of iron throughout the retina. There was an increase in Ft-L immunolabeling throughout the neurosensory retina in 2-week (Fig. 2E) and 5-month (Fig. 2G) MCA mice compared to age-matched controls (Fig. 2D, 2F). The increase in Ft-L immunolabeling in the MCA retinas was measured using pixel density quantification (Fig. 2H).

Retinal iron accumulation was also demonstrated by a decrease in the levels of transferrin receptor (Tfr) and divalent metal transporter 1 (Dmt1), components of the transferrin-bound iron (TBI) import system. An increase in cellular iron levels leads to a decrease in binding of IRP1 and IRP2 to the 3′ IRE on the mRNA transcripts of Dmt1 and Tfr, leading to mRNA instability and decreased protein production per transcript.[27] Previous work has shown that Dmt1 levels decrease in two

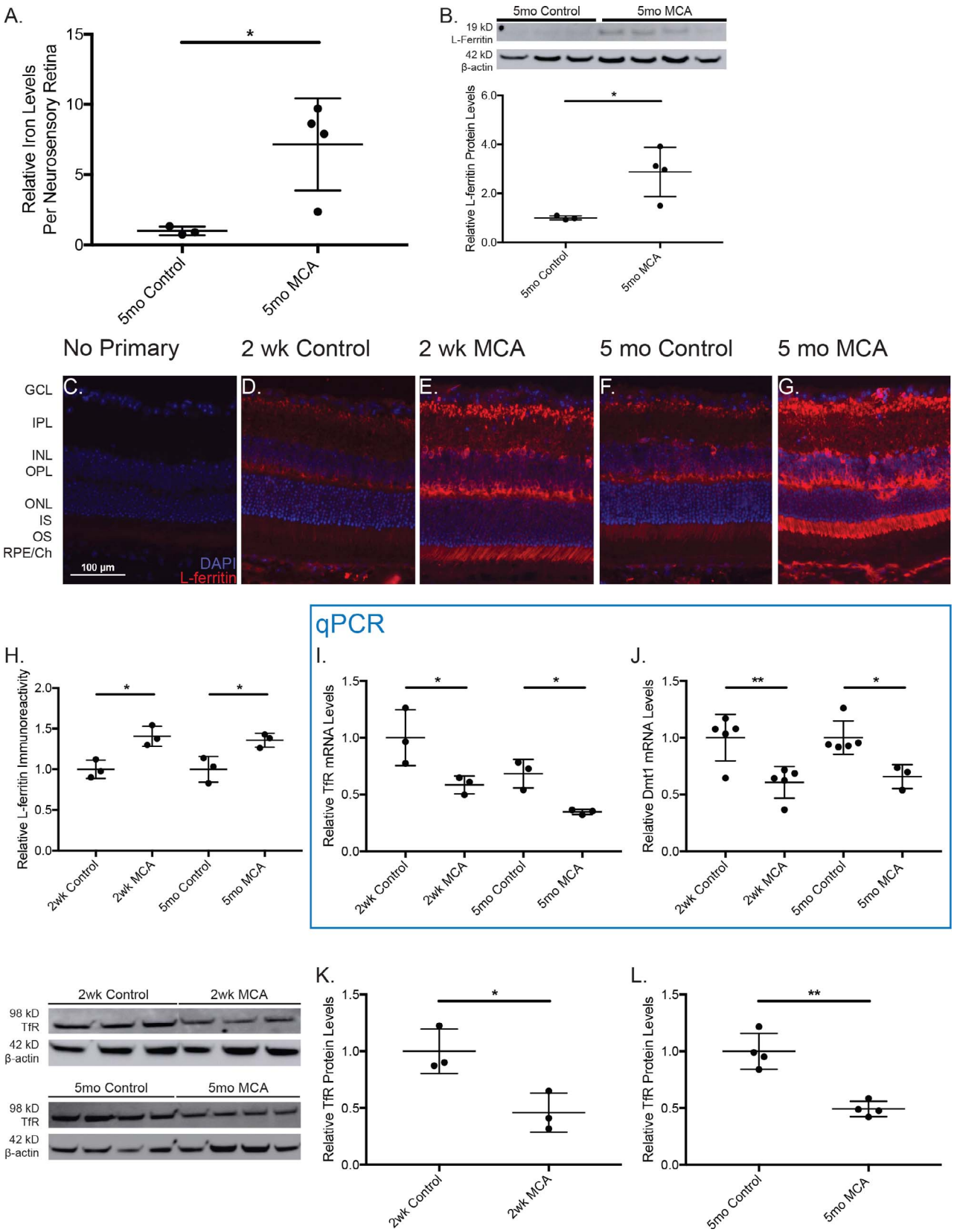

Figure 2. Primary Müller cell loss leads to retinal iron accumulation at 2 weeks and 5 months post MCA. iCP-MS for iron demonstrates that there are increased iron levels within the neurosensory retinas of the 5-month MCA mice compared to 5-month controls (**A**). $N = 3$ for 5-month control group, and $N = 4$ for 5-month MCA group. L-ferritin (Ft-L) protein levels within the neurosensory retina were assessed using Western analysis (**B**). There is an increase in Ft-L protein levels in the 5-month MCA retina compared with 5-month controls. Immunofluorescence for Ft-L demonstrates an increase in the expression of Ft-L in both the 2-week MCA (**E**) and 5-month MCA (**G**) retinas compared with age-matched controls (**D**, **F**). One representative photomicrograph for each group is shown. *Scale bars*: 100 μm. Changes in expression levels were quantified using pixel density

analysis (**H**). The mRNA levels of transferrin receptor (Tfr) (**I**) and divalent metal transporter 1 (Dmt1) (**J**) were significantly decreased in both the 2-week and 5-month MCA retinas compared with age-matched controls. Tfr protein levels decreased in both the 2-week MCA (**K**) and 5-month MCA (**L**) retinas compared with age-matched controls, as assessed by Western analysis. Loading control β-actin (42 kDa) bands are shown below each set of lanes. Plots of densitometry normalized to loading control calculated using FIJI software. Numbers represent mean values (±SEM). $^{*}P < 0.05$, $^{**}P < 0.01$. GCL, ganglion cell layer; IPL, inner plexiform layer; ONL, outer nuclear layer; INL, inner nuclear layer; IS, inner segments; OS, outer segments.

other models of retinal iron accumulation, Hepc KO and Cp/Heph Double KO mice.[23] We found that there was a decrease in the mRNA levels of Tfr (Fig. 2I) and Dmt1 (Fig. 2J) and a decrease in the protein levels of Tfr, as assessed by Western analysis, in the 2-week (Fig. 2K) and 5-month (Fig. 2L) MCA retinas compared with age-matched controls. These data demonstrate that beginning at 2 weeks post MCA, Müller cell loss leads to a disruption of retinal iron homeostasis and an increase in the intracellular iron levels within the neurosensory retina.

Primary Müller Cell Loss Does Not Affect the Production of the Iron Regulatory Hormone Hepcidin

Iron accumulation following MCA may be caused by loss of BRB integrity or may be due to changes in the level of hepcidin production by dysfunctional Müller cells. To determine whether changes in hepcidin production may be affecting retinal iron homeostasis in the MCA retinas, we investigated mRNA levels of hepcidin, as well as mRNA and protein levels of the iron importer Fpn and the associated multicopper ferroxidases, ceruloplasmin (Cp) and hephaestin (Heph). We found that there was no change in Hamp (hepcidin antimicrobial peptide) mRNA levels between the MCA and control mice at either time point (Fig. 3A). There was also no significant change in the Fpn mRNA levels in the MCA and control retinas at either time point (Fig. 3B). Additionally, there was no change in the mRNA levels of Heph (Fig. 3E) and Cp (Fig. 3F), multicopper ferroxidases that are necessary for ferroportin expression and function on the cell membrane[28,29] between the MCA and control mice at either time point. However, there was a significant increase in the protein level of Fpn in the 5-month MCA retinas compared with 5-month controls (Fig. 3D), but no change in protein levels 2 weeks post ablation, as assessed by Western analysis (Fig. 3C). The lack of change in hepcidin mRNA levels in the 2-week and 5-month MCA neurosensory retinas indicates that Müller cell loss does not significantly affect the production of hepcidin. The increase in Fpn protein but not mRNA levels in the MCA retina at the 5-month time point likely occurs in response to intracellular iron accumulation within the retina, as Fpn contains a 5′ IRE and is regulated by iron in the same way as Ft-L.[30]

Primary Müller Cell Loss Differentially Affects the Expression of Transferrin-Bound and Non-transferrin-Bound Iron Importers

In order for the Ft-L levels within the retina to increase, there needs to be an increase in the levels of intracellular iron, which can be achieved by an increase in the expression of iron importers on the cell membrane. There are two canonical pathways for cellular iron import—TBI and non-transferrin-bound iron (NTBI) import. There is a decrease in the levels of the two iron transporters involved in the TBI import pathway, Tfr and Dmt1, as these importers are negatively regulated by intracellular iron through the Irp-IRE pathway (Fig. 2I, J). Therefore, cellular iron import may be increased through the NTBI import pathway, which is governed by Zip8 and Zip14 iron importers. The cell-membrane levels of Zip8 and Zip14 are positively regulated by iron accumulation.[23,31,32]

We found that there is no change in the mRNA levels of Zip8 in the MCA and control retinas at either time point (Fig. 4A, E). There was also no change in Zip8 protein levels in the MCA and control retinas at the 2-week time point (Fig. 4C). However, there was an increase in Zip8 protein levels in the 5-month MCA retinas compared with controls (Fig. 4G). These data are consistent with other work, which suggests that Zip8 is positively regulated through a posttranscriptional mechanism in response to iron accumulation in a manner analogous to Zip14.[23,32] Unlike Zip8, Zip14 mRNA levels were affected by MCA. We found that there was a significant decrease in mRNA levels in the 2-week MCA retina compared with the 2-week controls (Fig. 4B) and no change in mRNA levels between the 5-month MCA and 5-month control retinas (Fig. 4F). There was also a significant decrease in Zip14 protein levels in the 2-week MCA retinas compared with 2-week controls as assessed by Western analysis (Fig. 4D), but no change in Zip14 protein levels between the 5-month MCA and 5-month control retinas (Fig. 4H).

Retinal Iron Accumulation in Human MacTel2 and Diabetic Retina

Müller cells are potential key mediators of several retinal diseases, including MacTel2 and DR, where loss of Müller cell–specific markers or signs of Müller cell stress have been noted.[6–10] The loss of Müller cells in these patients may lead to retinal iron dysregulation, which may in turn contribute to retinal degeneration. To determine whether patients with MacTel2 and DR have retinal iron accumulation, Perls' Prussian Blue stain was used to semiquantitatively assess macular iron levels in both a MacTel2 and DR patient. We found strong label in the RPE and outer plexiform layer of the DR patient (Fig. 5B) and strong iron labeling in the RPE of the MacTel2 patient (Fig. 5C) compared to the healthy age-matched control (Fig. 5A). The lack of signal in healthy controls is consistent with previously reported data from the retinas of elderly donors.[2]

Discussion

Retinal iron accumulation has been implicated in the pathogenesis of retinal degenerative diseases such as AMD, making it important to increase understanding of retinal iron regulation and transport. Müller cells are suspected to play a major part in the maintenance of retinal iron homeostasis for several reasons. They are critical for the formation and maintenance of the inner BRB. They express all the proteins involved in iron import and export and the iron regulatory hormone, hepcidin. Finally, their processes extend almost the entire thickness of the retina from the inner to the outer limiting membrane and contact all layers of retinal neurons, potentially allowing for distribution of iron across the neurosensory retina. We used the inducible transgenic model of primary Müller cell loss, developed by Shen et al.,[13] to demonstrate that Müller cell loss or dysfunction leads to iron

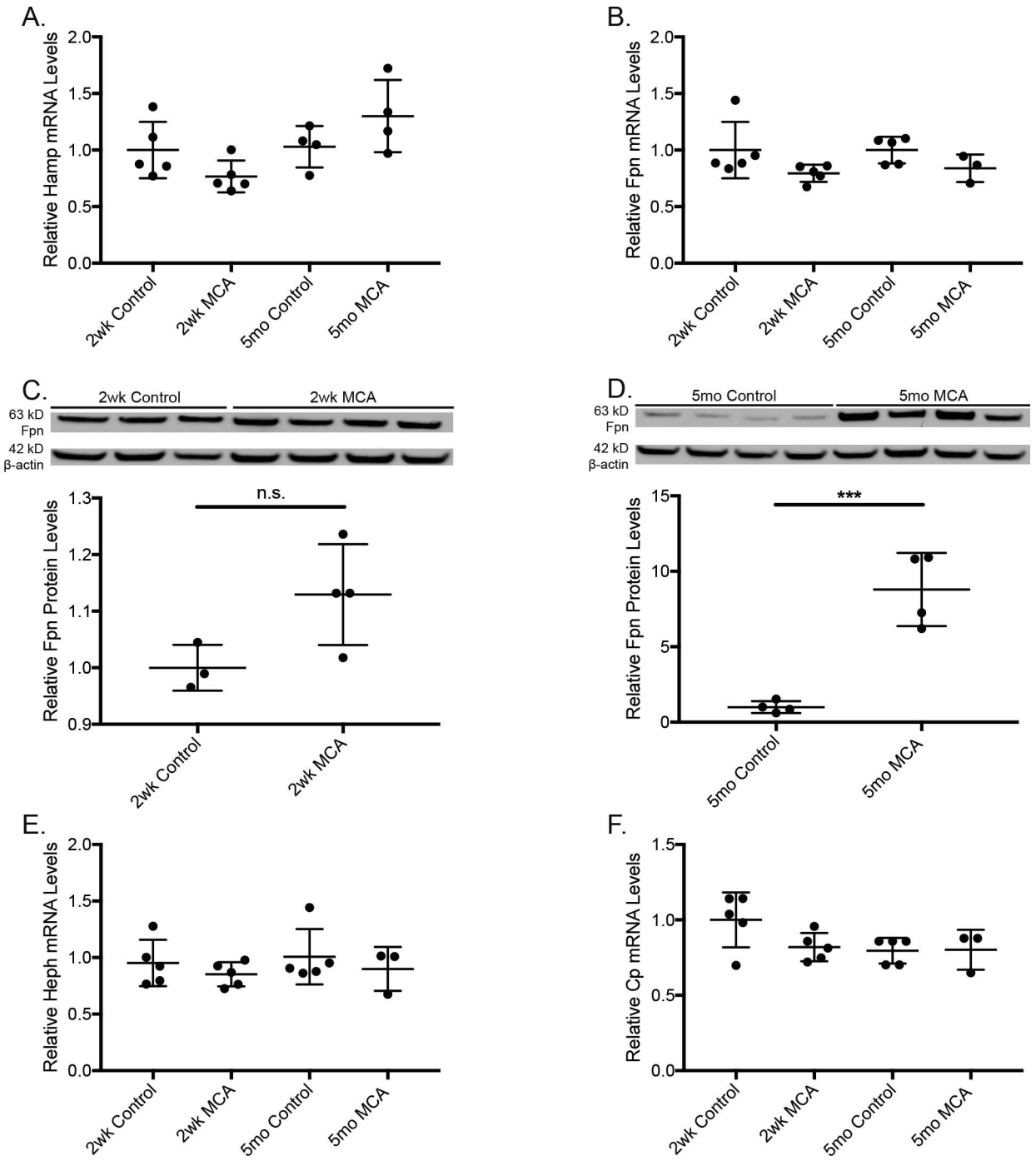

Figure 3. Primary Müller cell loss does not affect the mRNA levels of the iron regulatory hormone hepcidin, but does lead to an increase in the protein levels of the iron importer Fpn. Hepcidin (encoded by Hamp) (**A**) and Fpn (**B**) mRNA levels were not significantly different between the MCA and the control retinas at the 2-week and 5-month time points. Fpn protein levels were assessed by Western analysis. There was no change in Fpn protein levels between the 2-week control and 2-week MCA retinas (**C**), but there was a significant increase in Fpn protein levels in the 5-month MCA retina compared with 5-month control retina (**D**). Loading control β-actin (42 kDa) bands are shown below each set of lanes. The exposure time of the 2-week blot was half of the exposure time of the 5-month blot. Plots of densitometry were normalized to loading control calculated using image software. Graphs show mean values (+SEM). The mRNA expression of the multicopper ferroxidases, Heph (**E**), and Cp (**F**) was not significantly different between the MCA and control retinas at 2 weeks and 5 months post MCA. $^{***}P < 0.001$.

accumulation within the neurosensory retina. Furthermore, we demonstrate that retinal iron accumulation following MCA most likely occurs due to loss of BRB integrity.

The loss of Müller cells leads to retinal iron accumulation that is evident 2 weeks post MCA and continues at 5 months post MCA. iCP-MS was used to directly demonstrate that total iron levels were increased in the neurosensory retinas of MCA animals compared with controls. Intracellular iron levels within the neurosensory retina were also indirectly assessed by mRNA or protein levels of several iron-regulated proteins involved in intracellular iron storage, import, and export. There was an increase in the Ft-L protein throughout the neurosensory retina in the MCA mice at both the 2-week and 5-month time points. A decrease in TBI import is an adaptive

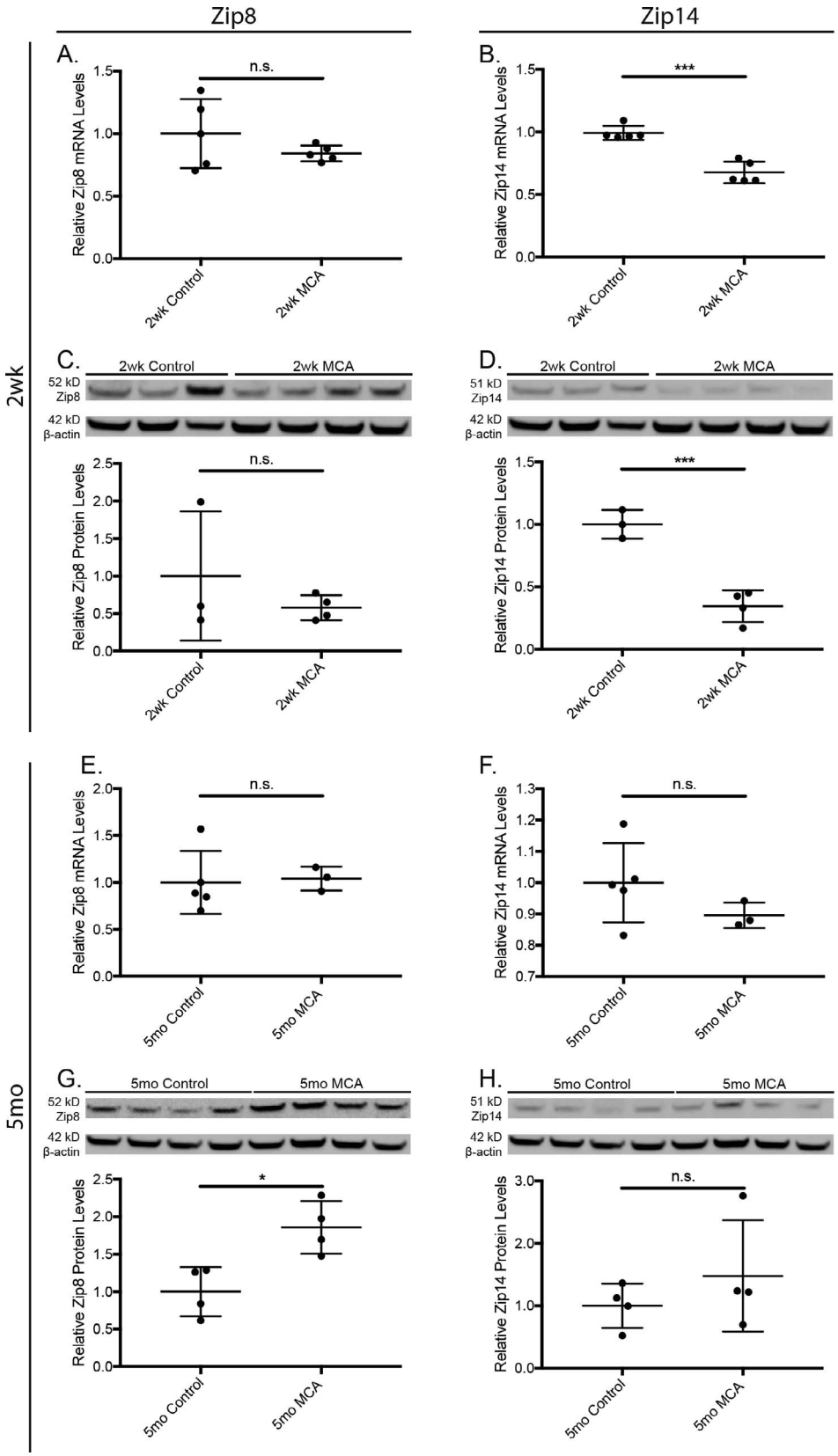

Figure 4. Iron accumulation in the primary MCA model leads to differential regulation of the NTBI importers Zip8 and Zip14. There is no change in Zip8 mRNA levels in the MCA and control retinas at 2 weeks (**A**) or 5 months (**E**) post ablation. There is no change in Zip8 protein levels between the MCA and control retinas at 2 weeks post ablation (**C**), but there is a significant increase in Zip8 protein levels in the MCA retinas compared with the control retinas at 5 months post ablation (**G**). There is a significant decrease in Zip14 mRNA levels between the MCA and control retinas at 2 weeks post ablation (**B**) but no change in Zip14 mRNA levels at 5 months post ablation (**F**). There is a significant decrease in Zip14 protein levels in the MCA retinas compared with controls at 2 weeks post ablation (**D**), but no change at 5 months post ablation (**H**). Loading control β-Actin (42kDa) bands are shown below each set of lanes. $^{*}P < 0.01$, $^{***}P < 0.001$.

Figure 5. Retinal iron accumulation in a patient with DR and a patient with MacTel2. Brightfield photomicrographs of Perls' stained macula sections show minimal label in a normal retina (**A**), show strong label in the RPE (*arrow*) and outer plexiform layer (*arrowhead*) compared to control from a patient with DR (**B**), and show strong label in the RPE (*arrow*) compared to control from a patient with MacTel2 (**C**).

response to an increase in iron levels to prevent further intracellular iron accumulation. Consistent with this regulatory mechanism, we found that there was a decrease in the mRNA levels of both Tfr and Dmt1 in the MCA retina at both the 2-week and 5-month time point. Additionally, we saw a decrease in the mRNA and protein levels of two components of the TBI import pathway, Tfr and Dmt1. These results are all consistent with an increase in retinal iron levels (Table).

The increase in ferritin levels throughout the neurosensory retina in the MCA mice indicates that Müller cell loss does not impede the ability of iron to enter the retina and be distributed to all retinal layers. If Müller cells were necessary for transporting iron to the retinal neurons, the loss or dysfunction of Müller cells in this model would lead to a dysregulation or loss of this process, most likely resulting in decreased Ft-L expression within retinal neurons. However, the overall increase in Ft-L expression throughout the neurosensory retina

Table. Normal Effect of Increased Iron on Iron-Handling Proteins and Effect of MCA on Iron-Handling Proteins at 2 Weeks and 5 Months Post Ablation

Protein	Normal Effect of Increased Iron on Iron-Handling Proteins	Reference	Observed Effect at 2 wk Post Ablation	Observed Effect at 5 mo Post Ablation
Ft-L	Decreased IRP binding to IRE in 5′ untranslated region (UTR) leads to increased Ft-L translation.	27	Increased immunoreactivity in MCA retina	Increased immunoreactivity and protein levels in MCA retina
Tfr	Decreased IRP binding to IRE in 3′ UTR leads to endonucleoytic cleavage and degradation of transcript.	27	Decreased mRNA and protein levels in MCA retina	Decreased mRNA and protein levels in MCA retina
Dmt1	Decreased IRP binding to IRE in 3′ UTR leads to endonucleoytic cleavage and degradation of transcript.	27	Decreased mRNA levels	Decreased mRNA levels
Fpn	1. Decreased IRP binding to IRE in 5′ UTR leads to increased Fpn translation. 2. Hepcidin binds to Fpn extracellular domain, leading to protein internalization and degradation.	18,30	No change in mRNA or protein levels in MCA retina	No change in mRNA levels, increased protein levels in MCA retina
Zip8	Increased protein levels, mechanism currently unknown, but is most likely similar to Zip14 iron regulation.	32	No change in mRNA or protein levels in MCA retina	No change in mRNA levels, increased protein levels in MCA retina
Zip14	Increased labile iron leads to glycosylation of membrane-bound Zip14, preventing internalization and degradation and resulting in a longer half-life of the protein on the cell membrane.	35	Decreased mRNA and protein levels in MCA retina	No change in mRNA or protein levels in MCA retina

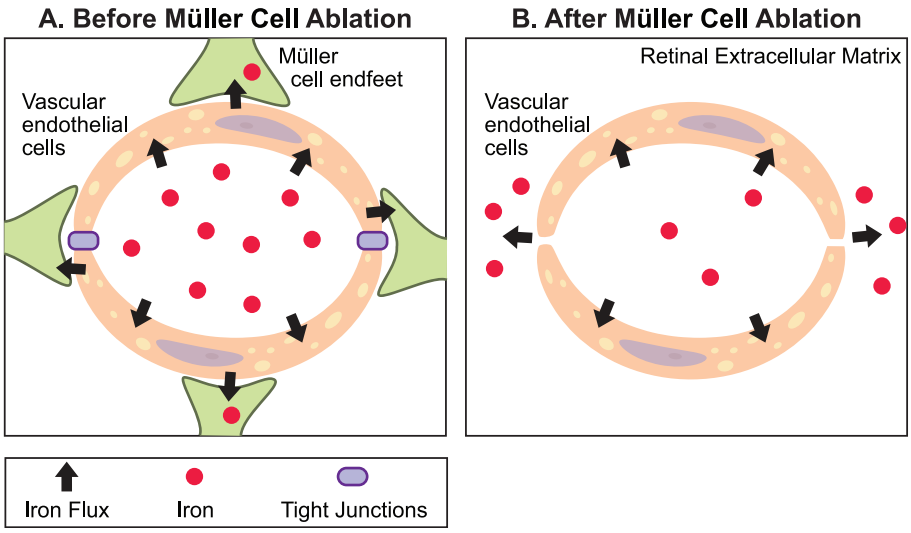

FIGURE 6. Proposed effect of Müller cell loss on inner BRB integrity. To get into the neurosensory retina, iron must be transported across the inner BRB, which consists of tight junctions formed between vascular endothelial cells and Müller cell endfeet (**A**). Following MCA, there is loss of inner BRB integrity, which results in unregulated flux of iron into the neurosensory retina, leading to an increase in iron throughout the neurosensory retina and the RPE (**B**).

does indicate that iron transport from the vascular endothelium into the retina is increasing when Müller cells are lost or dysfunctional. This may be due to a loss of the physical blockage of the inner BRB or due to an increase in iron import through vascular endothelial cells into the retina via Fpn. This second possibility was tested by assessing the effect of Müller cell loss on the mRNA levels of the iron regulatory hormone, hepcidin.

We did not see a change in the mRNA levels of hepcidin between the control and MCA mice at either time point. There was also no change in Fpn mRNA levels at either time point and no change in Fpn protein levels in the 2-week MCA and 2-week control retinas. However, there was an increase in Fpn protein levels in the 5-month MCA mice compared with 5-month controls. This pattern indicates that Fpn protein levels are increasing in the MCA retina at the later time point in response to the progressive retinal iron accumulation. This demonstrates that the increase in Fpn protein is an adaptive response by the retina to export intracellular iron and decrease retinal levels instead of a primary cause of retinal iron accumulation in response to a decrease in hepcidin expression. Taken together, these data demonstrate that iron accumulation is not caused by dysregulation of hepcidin.

We did, however, see evidence that loss of BRB integrity may be allowing unregulated iron entry into the retina. First, we demonstrated loss of BRB integrity by showing diffuse albumin staining throughout the neurosensory retina in the 2-week and 5-month MCA mice, while albumin was restricted to retinal blood vessels in the age-matched control mice. Second, we saw changes in the proteins levels of Zip14 and Zip8, two components of the NTBI import pathway that may indicate loss of BRB integrity.

The NTBI importers, Zip8 and Zip14, respond differently from TBI importers to increased iron levels. Zip8 and Zip14 are iron importers that are expressed on the cell surface. In hepatocytes, an increase in iron levels leads to an increase in the half-life of Zip14 on the cell membrane, leading to increased cellular iron import.[31] Likewise, iron accumulation in rat hepatoma cells leads to increased Zip8 cell-membrane expression.[32] Our lab has recently demonstrated that Zip8 and Zip14 protein levels within the retina are also positively regulated by an increase in retinal iron levels.[23] In the MCA model, retinal iron accumulation leads to an increase in Zip8 protein levels in the MCA retinas at the 5-month time point, as expected. However, there was a decrease in Zip14 protein levels. This could be explained due to different responses of Zip8 and Zip14 to changes in retinal holo-transferrin (holo-Tf) levels. An increase in holo-Tf within the retina leads to a decrease in Zip14 protein levels, but has no effect on Zip8 protein levels.[23] In the MCA model, the loss of BRB integrity may lead to an increase in holo-Tf within the retina, as holo-Tf is able to pass unregulated through the BRB. This could lead to the decrease in Zip14 protein levels seen in the 2-week MCA retinas compared with controls. We also see a decrease in Zip14 mRNA levels in the 2-week MCA retinas compared with controls. To the best of our knowledge there is no documented negative transcriptional regulatory mechanism of Zip14. Therefore, the decrease in Zip14 mRNA in response to MCA represents a novel regulatory pathway of Zip14 that needs to be explored further. At 5 months post MCA, there is additional iron accumulation within the neurosensory retina, leading to positive regulation of Zip14 on the cell membrane. The combination of positive regulation by the increase in iron levels and the negative regulation by the increase in holo-Tf levels may explain the lack of significant difference in Zip14 protein levels between the 5-month MCA and 5-month control retinas. Zip8 protein levels, however, are not affected by changes in holo-Tf levels and are therefore increased at 5-months post ablation due to the increase in retinal iron levels. The increase in the level of NTBI importer Zip8 could contribute to the increased intracellular iron levels in neurons, despite the decrease in the expression of TBI importers, if extracellular NTBI is available.

The lack of ferritin accumulation within Müller cells, the lack of change in hepcidin mRNA levels, the expression pattern of the NTBI importers in the context of retinal iron accumulation, along with the evidence of loss of barrier function in the MCA retina, all point toward loss of BRB integrity as the link between MCA and retinal iron dysregulation. The presence of Müller cell processes surrounding the vascular endothelium helps to limit the flow of iron into the retina. The loss of the inner BRB integrity in this model may lead to dysregulation of iron transport from the vasculature into the retina (Fig. 6).

Müller cell loss or dysfunction occurs in patients with MacTel2 and DR. Here, we demonstrate that the loss of BRB integrity in the MCA mice leads to retinal iron dysregulation. Retinal iron accumulation leads to oxidative injury, including photoreceptor degeneration, and presents a possible pathway for photoreceptor degeneration in retinal diseases involving Müller cell loss. We show that a patient with MacTel2 had increased iron levels within the RPE and a patient with DR had increased iron levels in the RPE and outer plexiform layer compared to an age-matched control, as assessed by Perls' stain. Our prior data suggest that iron flows from the neurosensory retina to the RPE.[19] Iron accumulation that results from loss of inner BRB integrity would lead to an initial increase in iron within the neurosensory retina. However, as the disease progresses and the patient ages, iron may be transported to the RPE. We believe that loss of BRB integrity secondary to Müller cell loss is leading to retinal iron accumulation in both the MacTel2 and DR patient. Differences in the spatial distribution of iron deposits in these two eyes may reflect the degree of retinal vascular leakage in the period prior to death. The increase in iron within the retina of MacTel2 and DR patients may contribute to the retinal degeneration associated with these diseases. These data indicate that preventing iron accumulation in patients with MacTel2 or DR, or removing some of the iron, may be a viable clinical measure to prevent subsequent retinal degeneration. The oral iron chelator, deferiprone, prevents retinal degeneration caused by retinal iron overload in several mouse models,[33,34] suggesting that long-term treatment with deferiprone or other iron chelators may be a preventive treatment for retinal diseases involving iron overload. Additionally, local ocular treatment with an iron chelator may address the concerns of using a systemic oral iron chelator.

In order to successfully treat retinal degenerative diseases, we must first understand the processes that contribute to degeneration. Müller cell loss or dysfunction is seen in several retinal degenerative diseases, but until recently, the downstream consequences of Müller cell loss or dysfunction have not been explored. Shen et al.[13] demonstrated that primary Müller cell loss may provide a link between vascular pathology and photoreceptor degeneration. In this study, we demonstrate that Müller cell loss or dysfunction leads to dysregulation of retinal iron homeostasis, leading to retinal iron accumulation. As iron accumulation leads to oxidative injury, dysregulation of retinal iron may represent one of the downstream effects of Müller cell loss that contributes to subsequent retinal degeneration.

Acknowledgments

Supported by National Institutes of Health/National Eye Institute Grant EY015240, the UPenn Vision Science Training Grant 5T32EY007035-37, Research to Prevent Blindness, the F.M. Kirby Foundation, a gift in memory of Lee F. Mauger, MD, and the Paul and Evanina Bell Mackall Foundation Trust.

Disclosure: **B. Baumann**, None; **J. Sterling**, None; **Y. Song**, None; **D. Song**, None; **M. Fruttiger**, None; **M. Gillies**, None; **W. Shen**, None; **J.L. Dunaief**, None

References

1. Beard J. Iron biology in function, muscle metabolism and neuronal functioning. *J Nutr*. 2000;131:697S–715S.
2. Hahn P, Milam A, Dunaief JL. Maculas affected by age-related macular degeneration contain increased chelatable iron in the retinal pigment epithelium and Bruch's membrane. *Arch Ophthalmol*. 2003;212:1099–1105.
3. Dunaief JL. Iron induced oxidative damage as a potential factor in age-related macular degeneration: the Cogan lecture. *Invest Ophthalmol Vis Sci*. 2006;47:4660–4664.
4. Newman E, Reichenbach A. The Müller cell: a functional element of the retina. *Trends Neurosci*. 1996;19:307–312.
5. Bringmann A, Pannicke T, Grosche J, et al. Müller cells in the healthy and diseased retina. *Prog Retin Eye Res*. 2006;24:397–424
6. Powner M, Gillies MC, Tretiach M, et al. Perifoveal Müller cell depletion in a case of macular telangiectasia type 2. *Ophthalmology*. 2010;117:2407–2416.
7. Powner M, Gillies MC, Zhu M, Vevis K, Hunyor AP, Fruttiger M. Loss of Müller's cells and photoreceptors in macular telangiectasia type 2. *Ophthalmology*. 2013;120:2344–2352.
8. Barber A, Antonetti DA, Gardner TW; for The Penn State Retina Research Group. Altered expression of retinal occluding and glial fibrillary acidic protein in experimental diabetes. *Invest Ophthalmol Vis Sci*. 2000;41:3561–3568.
9. Mizutani M, Gerhardinger C, Lorenzi M. Müller cell changes in human diabetic retinopathy. *Diabetes*. 1998;47:445–449.
10. Di Leo MA, Caputo S, Falsini V, Porciatti A, Greco V, Ghirlanda G. Presence and further development of retinal dysfunction after 3-year follow up in IDDM patients without angiographically documented vasculopathy. *Diabetologia*. 1994;37:911–916.
11. Fernandez-Sanchez L, Lax P, Campello L, Pinilla I, Cuenca N. Astrocytes and Müller cell alterations during retinal degeneration in a transgenic rat model of retinitis pigmentosa. *Front Cell Neurosci*. 2005;9:484.
12. Jones BW, Watt CB, Frederick JM, et al. Retinal remodeling triggered by photoreceptor degenerations. *J Comp Neurol*. 2003;464:1–16.
13. Shen W, Fruttiger M, Zhu L, et al. Conditional Müller cell ablation causes independent neuronal and vascular pathologies in a novel transgenic model. *J Neurosci*. 2012;32:15715–15727.
14. Zhao M, Andrieu-Soler C, Kowalczuk L, et al. A new CRB1 rat mutation links Müller glial cells to retinal telangiectasia. *J Neurosci*. 2005;35:6093–6106.
15. Tout S, Chan-Ling T, Holländer H, Stone J. The role of Müller cells in the formation of the blood-retinal barrier. *Neuroscience*. 1993;55:291–301.
16. Klaassen I, Van Noorden CJ, Schlingemann RO. Molecular basis of the inner blood-retinal barrier and its breakdown in diabetic macular edema and other pathological conditions. *Prog Retin Eye Res*. 2013;34:19–48
17. Gnana-Prakasam J, Martin PM, Smith SB, Ganapathy V. Expression and function of iron-regulatory proteins in retina. *IUBMB Life*. 2010;62:363–370.
18. Rivera S, Nemeth E, Gabayan V, Lopez MA, Farshidi D, Ganz T. Synthetic hepcidin causes rapid dose-dependent hypoferremia and is concentrated in ferroportin-containing organs. *Blood*. 2005;106:2196–2199.
19. Theurl M, Song D, Clark E, et al. Mice with hepcidin-resistant ferroportin accumulate iron in the retina. *FASEB J*. 2015;30:813–823.
20. Hadziahmetovic M, Song Y, Ponnuru P, et al. Age-dependent retinal iron accumulation and degeneration in hepcidin knockout mice. *Invest Ophthalmol Vis Sci*. 2010;52:109–110.
21. Konerirajapuram NS, Coral K, Punitham R, Sharma T, Kasinathan N, Sivaramakrishnan R. Trace elements iron, copper, and zinc in vitreous of patients with various vitroretinal disease. *Indian J Ophthalmol*. 2004;52:145–148.
22. Ciudin A, Hernandez C, Simo R. Iron overload in diabetic retinopathy: a cause or a consequence of impaired mechanisms? *Exp Diabetes Res*. 2010;2010:714108.

23. Sterling J, Guttha S, Song Y, Song D, Hadziahmetovic M, Dunaief JL. Iron importers Zip8 and Zip14 are expressed in retina and regulated by retinal iron levels. *Exp Eye Res*. 2017; 155:15–23.
24. Schindelin J, Arganda-Carreras I, Frise E, et al. Fiji: an open-source platform for biological-image analysis. *Nat Methods*. 2012;9:676–682.
25. Li Y, Song D, Song Y, et al. Iron-induced local complement component 3 (C3) up-regulation via non-canonical transforming growth factor (TGF)-β signaling in the retinal pigment epithelium. *J Biol Chem*. 2015;290:11918–11934.
26. Lewis GP, Fisher SK. Up-regulation of glial fibrillary acidic protein in response to retinal injury: its potential role in glial remodeling and a comparison to vimentin expression. *Int Rev Cytol*. 2003;230:263–290.
27. Rouault TA, Tang CK, Kaptain S, et al. Cloning of the cDnA encoding an RNA regulatory protein-the human iron-responsive element-binding protein. *Proc Natl Acad Sci U S A*. 1990; 87:7958–7962.
28. De Domenico I, Ward DM, Bonaccorsi di Patti MC, et al. Ferroxidase activity is required for the stability of cell surface ferroportin in cells expressing GPI-ceruloplasmin. *EMBO J*. 2007;26:2823–2831.
29. Jeong S, David S. Glycosylphosphatidylinositol-anchored ceruloplasmin is required for iron efflux from cells in the central nervous system. *J Biol Chemistry*. 2003;278:27144–27148.
30. Lymboussaki A, Pignatti E, Montosi G, Garuti C, Haile DJ, Pietrangelo A. The role of the iron responsive element in the control of ferroportin1/IREG1/MTP1 gene expression. *J Hepatol*. 2003;39:710–715.
31. Nam H, Wang CY, Zhang L, et al. Zip14 and DMT1 in the liver, pancreas, and heart are differentially regulated by iron deficiency and overload: implications for tissue iron uptake in iron-related disorders. *Haematologica*. 2013;98:1049–1057.
32. Wang CY, Jenkitkasemwong S, Duarte S, et al. Zip8 is an iron and zinc transporter whose cell-surface expression is up-regulated by cellular iron loading. *J Biol Chem*. 2012;287: 34032–34043.
33. Song D, Zhao L, Li Y, et al. The oral iron chelator deferiprone protects against systemic iron overload-induced retinal degeneration in hepcidin knockout mice. *Invest Ophthalmol Vis Sci*. 2014;55:4525–4532
34. Hadziahmetovic M, Song Y, Wolkow N, et al. The oral iron chelator deferiprone protects against iron overload-induced retinal degeneration. *Invest Ophthalmol Vis Sci*. 2011;53: 959–968.
35. Zhao N, Zhang AS, Worthen C, Knutson MD, Enns CA. An iron-regulated and glycosylation-dependent proteasomal degradation pathway for the plasma membrane metal transporter ZIP14. *Proc Natl Acad Sci USA*. 2014;111:9175–9180.

Investigative Ophthalmology & Visual Science